Impacts of a novel controlled-release TiO_2-coated (nano-) formulation of carbendazim and its constituents on freshwater macroinvertebrate communities

Nederstigt, Tom A.P.; Peijnenburg, Willie J.G.M.; Schrama, Maarten; van Ommen, J. Ruud; Vijver, Martina G.

DOI
10.1016/j.scitotenv.2022.156554

Publication date
2022

Document Version
Final published version

Published in
Science of the Total Environment

Science of the Total Environment 838 (2022) 156554

Contents lists available at ScienceDirect

Science of the Total Environment

journal homepage: www.elsevier.com/locate/scitotenv

Impacts of a novel controlled-release TiO_2-coated (nano-) formulation of carbendazim and its constituents on freshwater macroinvertebrate communities

Tom A.P. Nederstigt [a,*], Willie J.G.M. Peijnenburg [a,b], Maarten Schrama [a], J. Ruud van Ommen [c], Martina G. Vijver [a]

[a] Institute of Environmental Sciences, University of Leiden, Leiden, the Netherlands
[b] National Institute for Public Health and the Environment, Bilthoven, the Netherlands
[c] Department of Chemical Engineering, TU Delft Process & Product Technology Institute, Delft University of Technology, Delft, the Netherlands

HIGHLIGHTS

- Controlled-release (nano-)formulations have been suggested to reduce non-target impacts of pesticides on ecosystems
- A novel controlled-release (nano-)formulation of carbendazim ($nTiO_2$-coated carbendazim) was produced
- Long-term fate & impacts were assessed on naturally assembled freshwater macroinvertebrate communities
- $nTiO_2$-coated carbendazim induced similar impacts as conventional (un-coated) carbendazim
- Realistic concentrations of $nTiO_2$ induced negligible effects on all community parameters

GRAPHICAL ABSTRACT

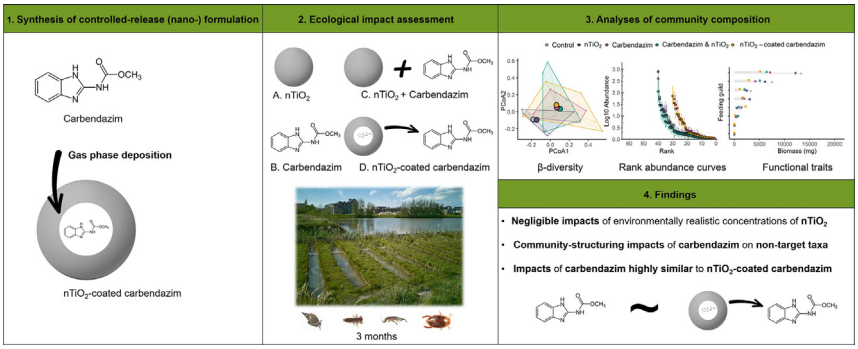

ARTICLE INFO

Editor: Daniel Wunderlin

Keywords:
TiO_2 nanoparticles
Pesticide
Gas phase deposition
Beta-diversity
Rank abundance
Mesocosm

ABSTRACT

Recently, the delivery of pesticides through novel controlled-release (nano-)formulations has been proposed intending to reduce (incidental) pesticide translocation to non-target sites. Concerns have however been raised with regards to the potentially enhanced toxicity of controlled-release (nano-)formulations to non-target organisms and ecosystems. We evaluated long-term (i.e. 1 and 3 month-) impacts of a novel controlled-release pesticide formulation (nano-TiO_2-coated carbendazim) and its individual and combined constituents (i.e. nano-sized TiO_2 and carbendazim) on naturally established freshwater macroinvertebrate communities. In doing so, we simultaneously assessed impacts of nano-sized TiO_2 ($nTiO_2$), currently one of the most used and emitted engineered nanomaterials world-wide. We determined ecological impacts on diversity (i.e. β-diversity), structure (i.e. rank abundance parameters), and functional composition (i.e. feeding guilds & trophic groups) of communities and underlying effects at lower organizational levels (i.e. population dynamics of individual taxa). Freshwater macroinvertebrate communities were negligibly impacted by $nTiO_2$ at environmentally realistic concentrations. The controlled-release (nano-)formulation significantly delayed release of carbendazim to the water column. Nevertheless, conventional- (i.e. un-coated-) and $nTiO_2$-coated carbendazim induced a similar set of adverse impacts at all investigated levels of ecological organization and time points. Our findings show fundamental restructuring of the taxonomic- and functional composition of macroinvertebrate communities as a result of low-level pesticide exposure, and thereby highlight the need for mitigating measures to reduce pesticide-induced stress on freshwater ecosystems.

* Corresponding author.
E-mail address: t.a.p.nederstigt@cml.leidenuniv.nl (T.A.P. Nederstigt).

http://dx.doi.org/10.1016/j.scitotenv.2022.156554
Received 31 March 2022; Received in revised form 2 May 2022; Accepted 4 June 2022
Available online 9 June 2022

1. Introduction

Freshwater ecosystems host near to 10 % of all described animal species on Earth and provide a plethora of services required to sustain human and environmental health (Maasri et al., 2022; Reid et al., 2019). Alarmingly, freshwater biodiversity has deteriorated at unprecedented rates over the last decades, with species losses exceeding those of both terrestrial and marine ecosystems (Albert et al., 2021; IPBES, 2019; Collen et al., 2009). Chemical stressors have long been recognized as prominent anthropogenic drivers underlying this deterioration, and as we have entered what is now being referred to as the 'Anthropocene', new and previously unrecognized pollutants and configurations of stress are emerging (Arthington, 2021; Reid et al., 2019; Crutzen, 2006). In cognizance of this, Persson et al. (2022) recently concluded that chemical pollution considered together with pollution by novel materials and modified biological lifeforms (collectively coined "novel entities") has surpassed its defined safe operating space within planetary boundaries.

Pesticides constitute a primary group of chemical pollutants and numerous studies over the past decades have documented their adverse effects on the physiology, functioning and diversity of non-target organisms and ecosystems (Brühl and Zaller, 2019). At the same time, their central role in current crop production strategies deems it unlikely that the use of pesticides is to be fully restricted in the coming decades (European Commission, 2020). As such, innovative methods which allow for chemical crop protection with minimal collateral environmental impacts could provide a rational means to ensure sufficient and more sustainable levels of agricultural production (Zhang et al., 2021).

To enhance efficacy of pesticides and mitigate environmental pollution resulting from their use, various studies have recently proposed the concept of controlled-release (nano-)formulations (Scott-Fordsmand et al., 2022; Zhang et al., 2021). In such formulations, active ingredients (i.e. pesticides) are encapsulated (e.g. by a film, capsule, or gel) with the aim to reduce runoff and more precisely control dosing at the target site (e.g. plant) over time (Kah et al., 2019; Sun et al., 2019). Controlled-release formulations are often categorized amongst nano-pesticides, and despite their intended reduced environmental impact, concerns have been raised about their enhanced toxicity towards non-target organisms and ecosystems (Zhang et al., 2021; Kah et al., 2019; Sun et al., 2019). These concerns predominantly revolve around potential toxicity of the used encapsulation material, enhanced bioavailability and reduced degradation rates of the active ingredient at non-target sites (Grillo et al., 2021).

When nano-sized encapsulation materials are used in controlled-release formulations, concerns about potential adverse environmental impacts can be regarded in parallel with those of nanomaterials (NMs) in general. To date, experimental data on NM toxicity is predominantly derived from short-term and small-scale laboratory experiments which focus almost exclusively on the physiology of individual species (Zheng & Nowack, 2021). Previous studies with conventional chemicals suggest however that such studies may hold little predictive power towards environmental impacts of stressors at higher levels of bio- and ecological organization (Barmentlo et al., 2019; Clement et al., 2012). As the current production and use of NMs is already resulting in their measurable presence in surface waters, there is a strong need for community-level assessments of their potential ecological impacts, both independently and as a constituent of controlled-release formulations of pesticides (Nabi et al., 2022; Peters et al., 2018).

In the present study, we aimed to assess impacts of a novel controlled-release (nano-)pesticide formulation and its constituents on freshwater macroinvertebrate communities. A controlled-release formulation consisting of a nano-sized-TiO_2 coating applied to the commonly used agricultural fungicide carbendazim was synthesized specifically for the purpose of the experiment using pulsed chemical vapor deposition (pCVD). We assessed individual and combined impacts of conventional (i.e. non-coated) carbendazim and nano-sized TiO_2 ($nTiO_2$) in parallel with the $nTiO_2$-coated product to determine the contribution of each constituent to observed effects. In doing so, we simultaneously performed an evaluation of community-level impacts of $nTiO_2$, currently one of the most widely used NMs globally, at environmentally relevant concentrations. The experiment was conducted over the course of 3 months in a series of outdoor experimental freshwater ditch ecosystems inhabited by naturally established ecological communities. Analysis of macroinvertebrate community parameters followed a step-wise approach to elucidate effects of the applied stressors on community diversity (i.e. β-diversity), structure (i.e. rank abundance parameters), functioning (i.e. feeding guilds & trophic groups) and underlying effects at lower organizational levels (i.e. population dynamics of individual species).

2. Materials & methods

2.1. Experimental site

The experiment was conducted at the 'Living Lab', an outdoor ecological research facility located in Oegstgeest, the Netherlands (SI Fig. A1, see http://mesocosm.org/ for an extensive description of the experimental site). The Living Lab consists of 36 artificial freshwater ditch ecosystems (used length-width-depth: 5-0.8-0.3 m; volume: 1200 L) each connected to an adjacent pond. Prior to the initiation of each experimental period, the connections to the adjacent pond are opened to allow for the natural establishment of ecological communities (i.e. microbes, plants and invertebrates). Since its founding in 2016, the experimental setup of the Living Lab has been used and validated extensively for the purpose of effect assessments of anthropogenic stressors on freshwater communities, and established communities have been found to exhibit high compositional similarity between ditches prior to application of treatments (Beentjes et al., 2021; Barmentlo et al., 2021; Barmentlo et al., 2019).

2.2. Experimental setup

Colonization took place via the adjacent pond over a period of 3 months (January 2019–March 2020) prior to the start of the experiment. Afterwards, each ditch was hydrologically isolated from the pond using acrylic barriers to eliminate the possibility of exchange of organisms, water and applied treatments, and established communities were left to settle for an additional month. Prior to application of the treatments, homogeneous establishment of ecological communities was assessed at all parameters measured throughout the experiment. Treatments were applied in May 2020 (described extensively in Section 2.3) and the experiment subsequently ran until September 2020. Physicochemical water quality parameters (temperature, pH, dissolved oxygen conductivity, NH^+_4, NO^-_3, chlorophyll A & turbidity) were measured on a weekly basis throughout the experimental period starting 2 weeks prior to treatment application (SI Table G1). Temperature, pH, conductivity and dissolved oxygen (DO) were measured using a Hach HQ40d multimeter (Hach Ltd., Colorado, USA) and NH^+_4 and NO^-_3 were measured using a Vernier LabQuest 3 multimeter (Vernier Software & Technology, Oregon, USA). Chlorophyll A and turbidity were measured using an AquaFluor® handheld fluorometer (Turner Designs, Inc., San Jose, USA).

2.3. Treatments & application

35 ditches were assigned to a control- and 4 treatment groups according to a systematic block design. All treatments were prepared and applied in replicates of 7 within a single day in early May 2020. Treatments consisted of nano-TiO_2-coated carbendazim (nTiO2-coated carbendazim) and its constituents (i.e. nano-sized TiO_2 and carbendazim) applied independently and in combination (i.e. nano-sized TiO_2 & carbendazim). Nominal concentrations of nano-sized TiO_2 ($nTiO_2$) treatments were 20 $\mu g\ L^{-1}$, which approximates measured concentrations of anthropogenic TiO_2 in European (0.2 to 8.1 $\mu g\ L^{-1}$; Peters et al., 2018) and North-American surface waters (~20 to 450 $\mu g\ L^{-1}$; Nabi et al., 2022). Carbendazim was applied at nominal treatment concentrations of 4 $\mu g\ L^{-1}$, aiming to achieve time-weighted average

(TWA) concentrations within the range of maximum permissible annual average surface water concentrations as set for the Netherlands at 0.6 μg L^{-1} (BKMW, 2009). This resulted in treatment concentrations of carbendazim representative of surface water concentrations globally (Alejandro et al., 2022; Wan et al., 2021; Merel et al., 2018). Nominal concentrations of the combined (i.e. $nTiO_2$ & carbendazim) and $nTiO_2$-coated carbendazim treatments were applied in accordance with carbendazim and $nTiO_2$ treatments, aiming to equalize total carbendazim (i.e. 4 μg L^{-1} starting concentration) and $nTiO_2$ (i.e. 20 μg L^{-1}) concentrations across all treatments.

2.3.1. $nTiO_2$-coated carbendazim

A $nTiO_2$-coated controlled-release product of carbendazim was prepared using pulsed chemical vapor deposition (pCVD), a gas phase deposition method. pCVD allows for layer-by-layer deposition of a metal oxide film (i.e. $nTiO_2$) of tens of nanometers onto dry particulates (i.e. in the current case carbendazim powder) resulting in a diffusion barrier through which the active ingredient is subsequently released. Gas phase deposition methods such as pCVD have been proposed as a viable option for producing controlled-release formulations of pharmaceuticals, and considering the similarities in desired properties of controlled-release pesticides, they could hold potential for their development as well (La Zara et al., 2021; Kääriäinen et al., 2017; Yan and Chen, 2015).

An extensive description of the applied pCVD process and methods used for characterization of the synthesized product and its environmental fate in the experimental setup are provided in SI B. In short, $nTiO_2$-coated carbendazim was synthesized by applying fifty pCVD cycles onto dry carbendazim powder (CAS no. 10605-21-7, 97 % purity, Sigma Aldrich, Missouri, USA) in a fluidized bed reactor (Zhang et al., 2019) using $TiCl_4$ and water as a reactants. Stock suspensions of $nTiO_2$-coated carbendazim were prepared immediately prior to treatment applications in 10 L of demineralized water under continuous (magnetic) stirring and subsequently distributed homogeneously across the surface of each ditch assigned to the $nTiO_2$-coated carbendazim treatment. Release of carbendazim from the $nTiO_2$-coated product was assessed over time in vitro in demineralized water by measuring absorption at 280–310 nm using UV–visible (UV–Vis) spectrophotometry and measurements of total available carbendazim (i.e. released and encapsulated into the $nTiO_2$ coating) in the $nTiO_2$-coated carbendazim treatments were performed in situ as described for un-coated carbendazim in Section 2.3.3.

2.3.2. $nTiO_2$

$nTiO_2$ (JRCNM01005a, European Commission – DG JRC, also provided by Degussa/Evonik as AEROXIDE P25®) was obtained from the repository for Representative Test Materials (RTMs) of the Joint Research Centre (JRC) of the European Commission. RTMs constitute accurate representations of industrially produced NMs and their use in nano-safety studies enhances comparability of results. The $nTiO_2$ used in the experiment has a reported particle size of 15–24 nm and consists of a mixture of ~85 % anatase: 15 % rutile crystalline structures (JRC, 2014). Anatase and rutile structures of $nTiO_2$ generally exhibit higher toxicity than amorphous structures (as formed in the pCVD product) (Clément et al., 2013). The use of anatase and rutile structures for the purpose of comparing impacts with the $nTiO_2$-coated product therefore serves as a worst-case scenario, and as described above, additionally ensures representativeness of $nTiO_2$ treatments to the wider range of products from which $nTiO_2$ is emitted to the environment.

Stock suspensions were initially prepared in 1 L of Mili-Q water (Milipore Milli-Q reference A + system, Waters-Millipore Corporation, Milford, MA, USA) followed by 10 min of ultra-sonication using a bath sonicator with a calculated energy output of 27 ± 0.2 W s^{-1} (Sonicor SC-50-22, Sonicor INC. NY, USA). Stocks suspensions were subsequently diluted in 10 L demineralized and applied to each ditch of the $nTiO_2$ and combined (i.e. $nTiO_2$ & carbendazim) treatment as described for the $nTiO_2$-coated carbendazim treatment (Section 2.3.1).

The size and shape of $nTiO_2$ were confirmed through Transmission Electron Microscopy (TEM, JEOL 1010, JEOL Ltd., Tokyo, Japan) (SI Fig. C1). Hydrodynamic diameters (z-average), polydispersity indices (PDIs), and zeta-potential were determined in 0.02 μm filtered ditch water using a Malvern Zetasizer Ultra (Malvern, Malvern, UK) (SI Table C1). To assure adequate count rates, samples were prepared and measured at test concentrations (i.e. 20 μg L^{-1}) and a concentration of 2 mg L^{-1}. Mass-based water column concentrations were determined from depth-integrated water samples collected across the length of each ditch after digestion in *aqua regia* (HNO_3 (65 %): HCL (37 %) = 1:3) using inductively-coupled plasma mass spectrometry (ICP-MS, PerkinElmer NexION 300D, Perkin Elmer, Massachusetts, USA). As ^{48}Ca is known to interfere with ^{48}Ti in elemental analysis and was expected to be present in our samples, reported concentrations are derived from ^{47}Ti isotope measurements. To account for background concentrations of [Ti] in our ditches, all reported concentrations were calculated by subtracting measured concentrations in ditches after treatment application from measured concentrations prior to treatment. Additional extensive characterization data has been made publicly available by the JRC (JRC, 2014).

2.3.3. Carbendazim

Carbendazim from the same batch as described for the pCVD preparation of $nTiO_2$-coated carbendazim was used to prepare stock solutions in 10 L of demineralized water for each ditch. Application to the ditches of the carbendazim and combined (i.e. $nTiO_2$ & carbendazim) treatments and subsequent collection of depth-integrated water samples followed the methodology as described for $nTiO_2$-coated carbendazim and $nTiO_2$ and (Sections 2.3.1 & 2.3.2). Samples were analyzed by a company specialized in trace analysis of agricultural chemicals after solid phase extraction using high performance liquid chromatography-tandem mass spectrometry (LC-MS/MS) using an in-house validated method (lower limit of detection: 0.01 μg L^{-1}).

2.4. Macroinvertebrate community sampling

Macroinvertebrate communities were sampled in all ditches one month prior to treatment (early May) and one (July) and three months (September) after treatment applications. To ensure standardization of collected samples, segments of one meter (measured in length, constituting a volume of approximately 140 L) were instantaneously closed off from the remainder of the ditch using a stainless steel barrier which was forced into the top sediment layer. Pelagic communities were subsequently sampled from the isolated section of each ditch using a dip net with a mesh size of 150 μm. Benthic communities were sampled from the same section by collecting the top 3–5 cm of sediment, which was sieved on a 500 μm stainless steel sieve from which all macroinvertebrates were collected. Any plant material present in samples was gently washed to ensure no macroinvertebrates were left out from the ultimate sample. Collection continued until subsequent samples (i.e. dip net sweeps) remained empty (i.e. no macroinvertebrates were observed). Identification and counting of specimens were performed at the field-laboratory unit on-site directly after sample collection to the lowest possible taxonomic level and all sampled organisms were returned to the respective ditches immediately after to minimize effects of sampling on the community composition. Highly abundant taxa (i.e. Gammaridae and Corixidae) were counted in homogenized subsamples and abundances were recalculated to the total sample volume. The timeframe between sample collection and return of the organisms to their respective ditch typically comprised 1–2 h per sample.

2.5. Statistical analysis

2.5.1. Effectiveness of macroinvertebrate community sampling

The effectiveness of the applied macroinvertebrate sampling strategy was assessed by generating species accumulation curves based on cumulatively collected samples per sampling time point. The sampling strategy was deemed sufficient (i.e. adequately representative of the community present in each ditch) when no newly identified taxon was observed per additionally collected sample. This was reached after collection of 20, 13 and 15

samples from the total of 35 ditches in May, July and September respectively (SI Fig. D1.).

2.5.2. Macroinvertebrate community dynamics – overview of analyses

Macroinvertebrate community analysis followed a 3-step approach which aimed to provide both detailed information on effects of treatments on individual taxa and their resulting effects on the structural and functional parameters of the community composition (outlined in detail in Sections 2.5.2.1–2.5.2.3). First, effects of treatments on taxonomic community diversity were assessed based on compositional dissimilarity measured using β-diversity indices (*β-diversity*, Fig. 1). Next, an explanatory analysis was performed in which the top contributing taxa to observed compositional dissimilarity were identified and analyzed to quantify differences in abundances between treatments and controls (*Explanatory analysis*, Fig. 1). Doing so provided insight into which taxa were predominantly affected by treatments and allowed for a qualitative comparison across treatments. Finally, a consequential analysis was performed that consisted of an evaluation of rank abundance curve (RAC) – related parameters and of the distribution of biomass per trophic group and feeding guild. This provided insight into the extent to which effects of treatments on compositional dissimilarity and taxon abundance/co-occurrence resulted in a shift in the underlying taxonomic- and functional community structure (*Consequential analysis*, Fig. 1). Data analysis was performed using R version 4.1.2 (R Core Team, 2017). Outcomes of statistical tests were considered statistically significant at $P < 0.05$.

2.5.2.1. Analysis of compositional dissimilarity (β-diversity indices). β-Diversity (or (dis)similarity-) indices provide a means to summarize and compare compositional differences between ecological communities based on their shared and unique taxa and (in some cases) homogeneity of abundances (Anderson et al., 2011). β-Diversity indices are calculated on the basis of comparisons between sets of communities/samples. When expressed as dissimilarity they yield a value bound between 0 (representing complete similarity) and 1 (representing complete dissimilarity) for each compared set of communities. Various β-diversity indices have been developed over the last decades, each differing in the weight that is attributed to specific aspects of community composition. As such, the use of different β-diversity indices can provide distinct insights into which of such aspects is the predominant driver of dissimilarity between communities of interest.

In the current study, dissimilarity in macroinvertebrate community structure between treatments and controls was assessed on the basis of the Bray-Curtis index calculated using raw- and log10(x + 1) transformed abundance data and the Sørensen dissimilarity index (see SI Table E1 for respective equations).The Bray-Curtis index accounts for both uniformity of abundances of taxa and the ratio between shared and unique taxa (i.e. differences in presence/absence of taxa) across compared communities (i.e. treatments), whilst the Sørensen index accounts for the latter only. As such, Sørensen dissimilarity between treatments is an indication of taxonomic turnover (i.e. the difference in unique and shared taxa between communities), whilst Bray-Curtis dissimilarity provides an aggregated measure which could also solely indicate differences in abundances of taxa between communities. Furthermore, the contribution of individual taxa in dissimilarity calculated according to the Bray-Curtis index is skewed towards taxa that are more abundant (see equation in SI Table E1). When differences in less abundant taxa are of interest as well, this can be mitigated by log10(x + 1) transformation of abundance data, effectively resulting in the down-weighing of highly abundant taxa in overall calculated dissimilarity (Tebby et al., 2017).

Differences in community dissimilarity between treatments and controls were assessed by permutational analysis of variance (PERMANOVA, function 'adonis2', R package 'Vegan'). To account for the applied systematic block design and the potential presence of a spatial gradient across the experimental setup, permutations were restricted between ditches of the same block. Post-hoc testing to compare individual treatments and treatments to control was done by subsetting datasets and selecting only relevant contrasts, after which the same procedure was followed as for the full datasets. Differences in homogeneity of multivariate dispersions (i.e. β-dispersion) between treatments were assessed through a permutation-based test of multivariate homogeneity of group dispersions (function 'permutest', R package 'Vegan'). Although homogeneity of multivariate dispersions has been suggested as an assumption for the validity of PERMANOVAs, Anderson and Walsh (2013) demonstrated that this is incorrect when study designs are balanced, as in the current experiment.

2.5.2.2. Explanatory analysis of compositional dissimilarity. Coefficients of each generated PERMANOVA model were extracted to identify the 10 taxa contributing most to observed dissimilarity between treatments. Differences in abundances of these taxa between respective treatments and controls were analyzed using Anova/Kruskall Wallace tests depending on whether assumptions for parametric models were met. Data and models were checked for heteroskedasticity (Levenes test) and normal distribution (Shapiro Wilk test and visual inspection of histograms and QQ-plots) of the residuals. When assumptions for homogeneity of variance were not met, Brown-Forsythe tests were performed. When assumptions for normality of residuals were not met, Kruskal-Wallis tests were performed followed by Bonferonni corrected Dunn's post-hoc tests.

2.5.2.3. Consequential analysis - rank abundance curves & representation of feeding guilds/trophic groups. Rank abundance curves (RACs) were generated using raw and log10(x + 1) transformed data. Differences in taxon richness, evenness and rank- and curve shape were calculated for each time point between treatments and controls (functions: 'RAC_difference' & 'RAC_change', R package: 'codyn') and analyzed using ANOVA's followed by Tukey pairwise comparisons. Differences in gains and losses of taxa (i.e. turnover) were analyzed over time using two-way anovas followed by Tukey pairwise comparisons. An overview of all assessed parameters and their calculation is provided in SI Table F1. All RAC related parameters were assessed as pre-set in the 'codyn' package. Therefore, log10(x + 1)

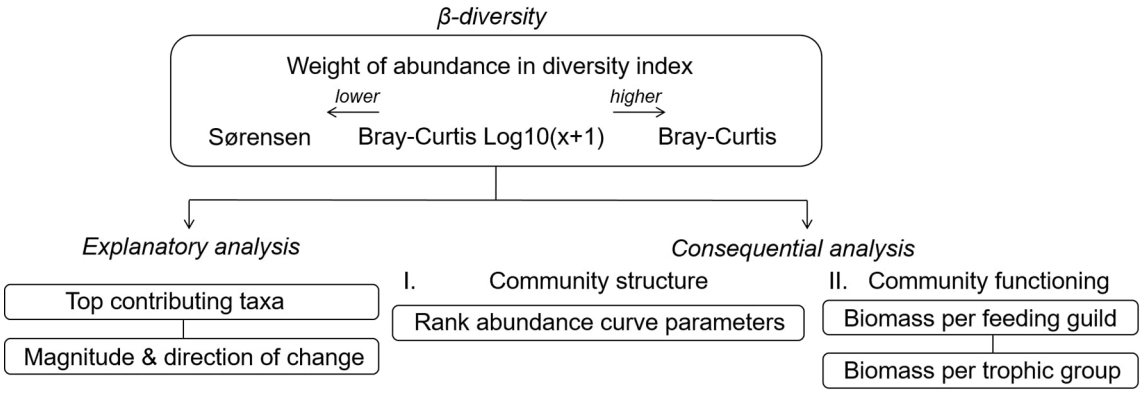

Fig. 1. Overview of the 3-step approach applied to macroinvertebrate community analysis in the experiment.

transformation of count data was only applied in calculating evenness, as transformation would not affect other metrics. Assumptions for data and models were assessed as described in Section 2.5.2.3.

Identified taxa were assigned to feeding guilds and trophic groups based on trait modalities derived from the Freshwater Ecology Database (Schmidt-Kloiber and Hering, 2015) according to Barmentlo (2020). Trait modalities were averaged for all available species in the identified taxonomic group when identification was not performed until species level. As abundance constitutes a poor estimation of actual biological representation of trait modalities, all count data was transformed to biomass. To do so, mass-length relationships were calculated according to Sabo et al. (2002) using values for maximum body length derived from the Freshwater Ecology Database. In case such data were not available in the Freshwater Ecology Database this was obtained from identification literature. Feeding guilds constituted gather-collectors, shredders, grazers, deposit feeders, filter feeders, predators & parasites, and biomass per feeding guild was calculated based on the reported percentage of representation of a taxon per guild. As such, the biomass of a single taxon was partitioned over all its assigned feeding guilds. Trophic groups were divided into herbivores, detritivores, omnivores and predators. Taxa were assigned to trophic groups in a binary manner, e.g. including only taxa which are specialized herbivores in the Herbivore group, and taxa which comprise multiple groups in the Omnivores group. Biomass data per feeding guild/trophic group and time point was subsequently analyzed as described for abundance data of individual taxa in Section 2.5.2.1. Analyses were performed on comparisons of absolute- and relative (i.e. to total) biomass per feeding guild/trophic group. This provided measures of both shifts in biomass per feeding guild/trophic group and their relative representation in the total ecosystem.

3. Results & discussion

3.1. Exposure characterization of $nTiO_2$

Particles used in the $nTiO_2$ treatments exhibited an average diameter of 24 ± 5 nm (mean ± standard deviation measured over 15 particles/aggregates) and a predominantly angular shape (SI Fig. C1). Introduction of $nTiO_2$ into ditchwater initially resulted in rapid aggregation (average hydrodynamic size immediately after preparation of suspensions 474 ± 111 nm). This was followed by stabilization of average hydrodynamic sizes over the course of 30 days of incubation (SI Table C1). Nevertheless, measurements of ζ potential (−7.2 ± 1.5 mV) and polydispersity indicated that although average hydrodynamic sizes remained stable, $nTiO_2$ was present in a broad range of particle sizes (SI Table C1).

Application of $nTiO_2$ resulted in initial measured water column concentrations of 23.6 ± 4.4 μg L^{-1} (mean ± standard error), thus ranging between 96 and 140 % of nominal treatment concentrations (Fig. 2A). Water column concentrations of $nTiO_2$ subsequently dissipated over time and stabilized between 30 (May) and 90 (September) days post treatment application at 7.5 ± 0.9 μg L^{-1}. As a result, time weighted average (TWA) $nTiO_2$ concentrations in the water column calculated over the entire timeframe of the experiment were 8.8 ± 0.3 μg L^{-1}. Observed aggregation (in)stability of $nTiO_2$ incubated in ditchwater in vitro indicated that initial dissipation of $nTiO_2$ from the water column in the experimental setup was likely due to aggregation occurring immediately after application of the treatments, followed by sedimentation of larger $nTiO_2$ aggregates. Aggregation and sedimentation of $nTiO_2$ is commonly observed in ecotoxicological studies performed at the laboratory scale, both in simulated (Nederstigt et al., 2022) and natural test media (Brunelli et al., 2013). Laboratory-scale ecotoxicological studies of $nTiO_2$ (and other poorly soluble NMs) however rarely consider subsequent stabilization of water column concentrations over longer periods as was observed in the current study. Instead, the test medium in laboratory-based ecotoxicological studies of NMs is often replaced at frequent intervals, as prescribed in various regulatory test-guidelines for NMs (OECD, 2021; OECD, 2017). This inherently results in a sequence of short-term exposure periods which are subsequently used to assess long(er) term responses. The findings of the current experiment suggest however that over longer timescales, water column exposure of $nTiO_2$ may be represented more realistically by relatively stable water column concentrations which can be ascribed to smaller aggregate sizes remaining in suspension.

3.2. Exposure characterization of carbendazim and $nTiO_2$-coated carbendazim

Water column concentrations of carbendazim measured immediately after application of the treatments were 4.0 ± 0.7 μg L^{-1} in the ditches of the carbendazim treatment and 4.1 ± 0.4 μg L^{-1} in the ditches of the combined (i.e. $nTiO_2$ & carbendazim) treatment (Fig. 2B & C). Concentrations subsequently dissipated rapidly in both treatments, to the point of reaching the analytical detection limit 90 days after treatment application (i.e. 0.01 μg L^{-1}) (Fig. 2B). This resulted in TWA concentrations of 0.15 ± 0.01 μg L^{-1} and 0.18 ± 0.01 μg L^{-1} for carbendazim and combined treatments respectively. Reported half-lives of carbendazim in freshwater systems range between around 15–60 days, which suggests that despite a (log) octanol-water partitioning coefficient (log K_{ow}) of 1.36, sorption to sediment likely played a partial role in the initially observed rapid dissipation of carbendazim from the water column (WHO Working Group, 1993).

TEM analysis of synthesized $nTiO_2$-coated carbendazim showed that particles were polydisperse and irregularly shaped, with sizes ranging between 100 and 500 μm (SI Fig. C2). The obtained $nTiO_2$ film on the final $nTiO_2$-coated carbendazim product significantly prolonged the release of carbendazim to the surrounding medium (SI Fig. C3). Initial release (i.e. <1 day) of carbendazim was more rapid than observed subsequently, suggesting that part of the carbendazim was not fully coated. Overall diffusion from the product was however significantly delayed, resulting in incomplete (~40 %) release over the course of the in vitro assay.

Initial measured concentrations of total carbendazim in $nTiO_2$-coated carbendazim treatments were 2.9 ± 0.3 μg L^{-1}, and TWA concentrations

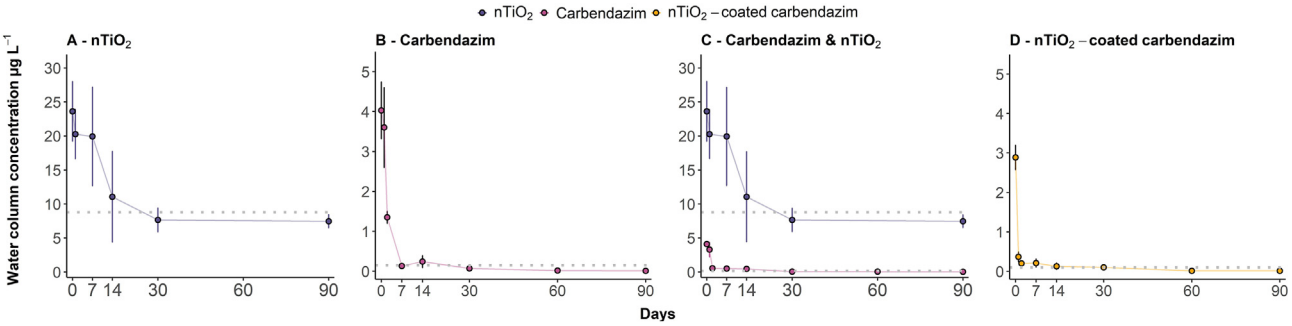

Fig. 2. Water column concentrations (mean ± standard error) of applied treatments across the timeframe of the experiment. Dotted grey lines represent time-weighted average concentrations. Treatments were added at day 0 (May), and days 30 (July) and 90 (September) are equivalent to macroinvertebrate sampling moments July and September. $nTiO_2$-coated carbendazim concentrations are expressed as total carbendazim concentrations (i.e. released & retained carbendazim). $nTiO_2$ concentrations in combined treatments (i.e. $nTiO_2$ & carbendazim) are duplicated from those as measured in $nTiO_2$ treatments, as differences in this regard were not expected.

were 0.10 ± 0.01 μg L^{-1}. This respectively constituted approximately 25 and 33 % lower concentrations than those measured in un-coated carbendazim treatments. Analysis of stock suspensions indicated that a total mass of carbendazim was added to the diches which was equivalent to 114 % of the intended treatment concentration (i.e. 4 μg L^{-1}). As such, it is likely that this discrepancy was predominantly caused by a combination of aggregation (i.e. by increasing heterogeneity of total carbendazim in the water column) and enhanced sedimentation.

3.3. Impacts of treatments on macro-invertebrate communities

Analysis of all assessed community parameters indicated that ditches assigned to respective treatments and controls exhibited high compositional similarity prior to treatment applications, and no statistically significant differences between any of the assigned groups (i.e. treatments) were observed (SI Table H1, I1, J1 & J2). The number of identified taxa across all treatments was 68 for May, 55 for July and 57 for September.

3.3.1. Compositional dissimilarity (β-diversity indices) & explanatory analysis

Macroinvertebrate communities in $nTiO_2$-coated carbendazim, carbendazim and combined (i.e. $nTiO_2$ & carbendazim) treatments displayed dissimilarity from controls for multiple β-diversity indices (Fig. 3, SI Table H1). One month after treatment application (July), this was observed in $nTiO_2$-coated carbendazim and carbendazim treatments for Bray-Curtis dissimilarity calculated using log10(x + 1) abundance data ($nTiO_2$-coated carbendazim: $F_{1,13} = 2.57$, $p = 0.02$; carbendazim: $F_{1,13} = 2.30$, $p = 0.02$) and for Sørensen dissimilarity ($nTiO_2$-coated carbendazim: $F_{1,13} = 3.20$, $p = 0.02$; carbendazim: $F_{1,13} = 2.10$, $p = 0.04$). Interestingly, combined treatments in July only displayed dissimilarity from controls when calculated according to the Sørensen index ($F_{1,13} = 1.74$, $p = 0.03$). The Sørensen index solely accounts for the ratio of unique and shared taxa (i.e. taxonomic turnover) between compared communities, whilst the Bray-Curtis index additionally considers heterogeneity of abundances of taxa. In addition, weights of all taxa are partitioned evenly in the calculation of the Sørensen index, whilst in the Bray-Curtis index

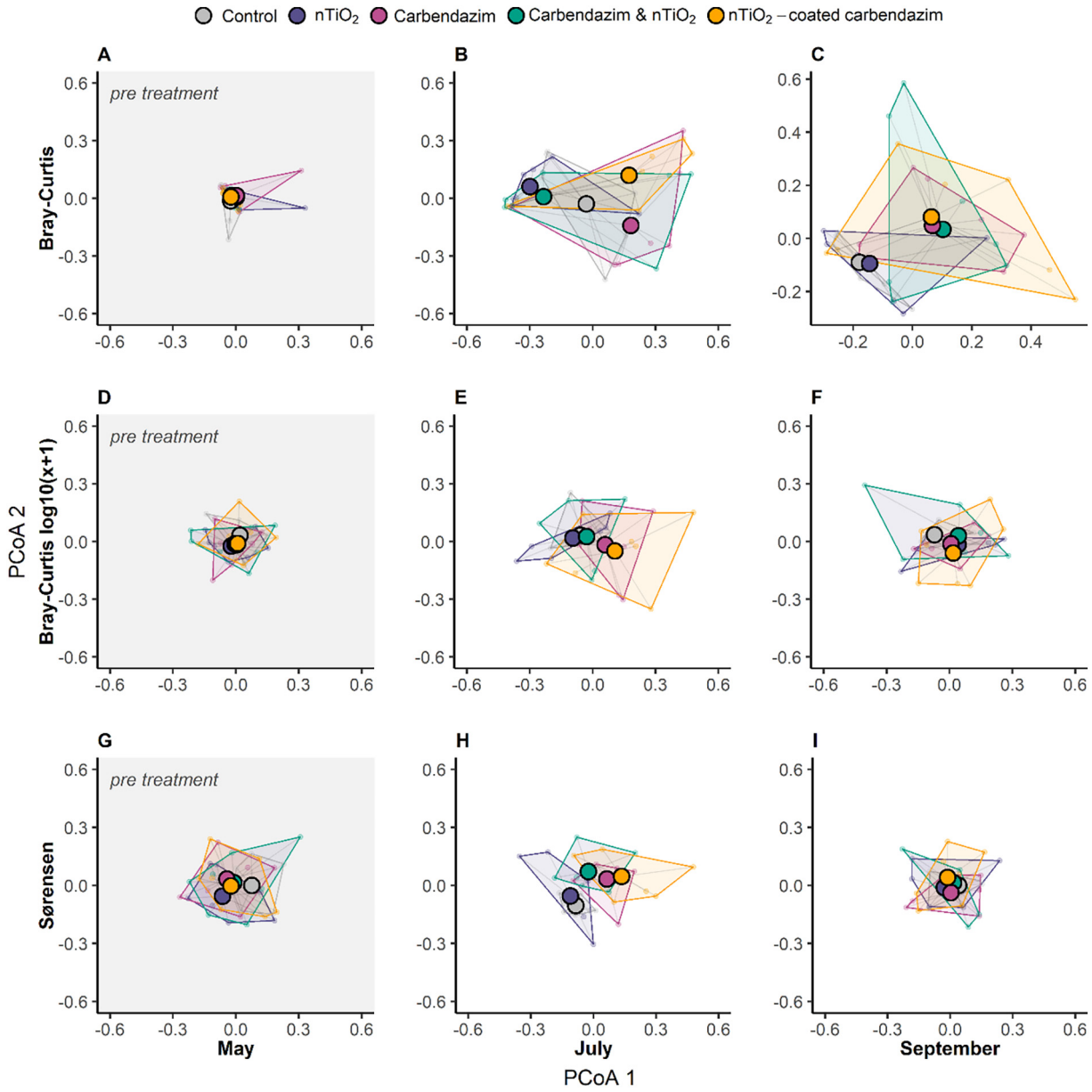

Fig. 3. Principle coordinate analysis plots (PCoAs) of each calculated β-diversity index per month. May = 1 month pre-treatment application, July = 1 month post treatment application and September = 3 months post treatment application. Centroids represent mean dissimilarity values per treatment and hulls are drawn around dissimilarity values of individual replicates (i.e. ditches).

more abundant taxa are weighed proportionally more than less abundant taxa. Although Sørensen dissimilarity thus indicated equivalent differences from controls in $nTiO_2$-coated carbendazim, carbendazim and combined treatments in terms of taxonomic turnover, in Bray-Curtis dissimilarity calculated between controls and combined treatments this difference was concealed by more even abundances of the remaining (and more highly abundant) taxa. Likewise, the absence of dissimilarity from controls in Bray-Curtis indices calculated using raw abundance data suggests that highly abundant taxa differed less in their relative abundance between $nTiO_2$-coated carbendazim, carbendazim and combined treatments and controls than lowly abundant taxa. The results of the explanatory analysis of top contributing taxa and differences in their abundances between treatments and controls underline this, as can be seen in abundance distributions in SI Figs. H2–H4.

Macroinvertebrate communities in all carbendazim-including treatments remained to display dissimilarity from controls three months (September) after treatment application (Fig. 3C). In contrast to observations for July, dissimilarity from controls was more pronounced when calculated according to the Bray-Curtis index using raw abundance data ($nTiO_2$-coated carbendazim: $F_{1,13} = 3.00$, $p = 0.03$; carbendazim: $F_{1,13} = 3.89$, $p = 0.02$; combined: $F_{1,13} = 12$, $p = 0.06$). Subsequent evaluation of top contributing taxa indicated larger differences in abundances than observed for July (SI Figs. H6–H8). In addition to observations of less pronounced community dissimilarity calculated according to the Sørensen index ($nTiO_2$-coated carbendazim: $F_{1,13} = 1.15$, $p = 0.27$; carbendazim: $F_{1,13} = 0.29$, $p = 1.00$; combined: $F_{1,13} = 0.26$, $p = 0.98$;) and the Bray-Curtis index based on log10(x + 1) abundance data ($nTiO_2$-coated carbendazim: $F_{1,13} = 1.81$, $p = 0.08$; carbendazim: $F_{1,13} = 1.60$, $p = 0.08$; combined: $F_{1,13} = 0.64$, $p = 0.87$), this indicates that taxonomic turnover now contributed less, and differences in abundance (of highly abundant taxa) contributed more to observed dissimilarity from controls.

Whilst macroinvertebrate communities in all carbendazim-including treatments thus displayed pronounced and largely equivalent dissimilarity from controls, this was not observed for $nTiO_2$ treatments (Fig. 3). A statistically significant difference ($F_{1,13} = 1.75$, $p = 0.04$) from controls was only detected for Bray-Curtis dissimilarity calculated using raw abundance data three months after application of the treatments (September). Principle coordinate analysis plots (PCoAs) indicated that this could largely be attributed to a single replicate of the $nTiO_2$ treatment which showed disproportionally high dissimilarity relative to controls in comparison to other replicates, deeming it unlikely that this resulted from application of $nTiO_2$ treatments (Fig. 3, SI Table H1).

Although multivariate measures such as β-diversity indices allow for making standardized and meaningful comparisons between communities, they can also result in abstraction and provide little information regarding the processes which may underlie differences between compared communities (Avolio et al., 2021; Avolio et al., 2019; Socolar et al., 2016). In the current experiment, decomposition of models based on appropriately selected β-diversity indices into their top contributing taxa and subsequent taxon-by-taxon analysis constituted a first step into mitigating this abstraction and to enhancing transparency regarding the community parameters driving dissimilarity. As such, it could be pinpointed that communities in $nTiO_2$-coated carbendazim, carbendazim and combined treatments showed highly similar responses, which resulted in quantitatively (i.e. in terms of abundance and aggregated diversity indices) and qualitatively (i.e. in terms of responding taxa) similar community dynamics over time.

3.3.2. Rank abundance curve parameters (RACs)

RACs of macroinvertebrate communities showed similar shapes and structures prior to application of treatments (Fig. 4A). Overall, communities displayed unevenness through high abundances in few, and low abundances in many taxa, as is more often observed in early succession stages of ecological communities such as in the experimental setup (Wang et al., 2021).

In concurrence with observations from β-diversity indices, RACs of $nTiO_2$-coated carbendazim, carbendazim and combined treatments deviated from those of controls both one (July) and three months (September) after treatment application (Fig. 5, SI Table I1). Overall taxonomic richness in $nTiO_2$-coated carbendazim and carbendazim treatments was reduced by ~15 % in both treatments in July ($nTiO_2$-coated carbendazim: Tukey $p = 5.6e^{-3}$; carbendazim: Tukey $p = 3.2e^{-4}$) and September ($nTiO_2$-coated carbendazim: Tukey $p = 8.2e^{-4}$; carbendazim: Tukey $p = 0.07$) (Fig. 5A). In July, this difference was observed to a lesser extent in combined treatments, (Tukey $p = 0.41$) whilst in September (combined: Tukey $p = 3.9e^{-5}$) all three carbendazim-including treatments showed similar deviations from controls (Fig. 5A). Reductions in abundances of highly ranked taxa of all carbendazim-including treatments also resulted in increases in evenness relative to controls, although this only resulted in statistically significant differences in carbendazim treatments in July (Dunnet $p = 0.01$) (Fig. 5B, SI Table I1).

The loss of lowly abundant taxa and reductions in numbers of highly abundant taxa culminated in differences in curve shape (i.e. curve area) in September (Fig. 5D) and taxa ranks (i.e. the abundance-determined rank position of taxa in the community) in all three carbendazim-including treatments in both July and September (Fig. 5C, SI Table I1). This process also referred to as taxa- or species reordering, occurred in absence of significant gains and losses of species over time, indicating that taxa reordering within carbendazim-including treatments was driven by changes in abundances (Fig. 5E, SI Table I1). Taxa reordering is thought to constitute a sensitive reflection of internal community dynamics, and differences in rank positions are expected to hold most significance with regard to community composition and ecosystem functioning when they involve extremes (e.g. a taxon which is amongst the lower ranks in one community, and amongst the higher ranks in the other, and vice versa) (Avolio et al., 2021; Avolio et al., 2019). In the current experiment, abundance-determined rank positions in treatments relative to controls

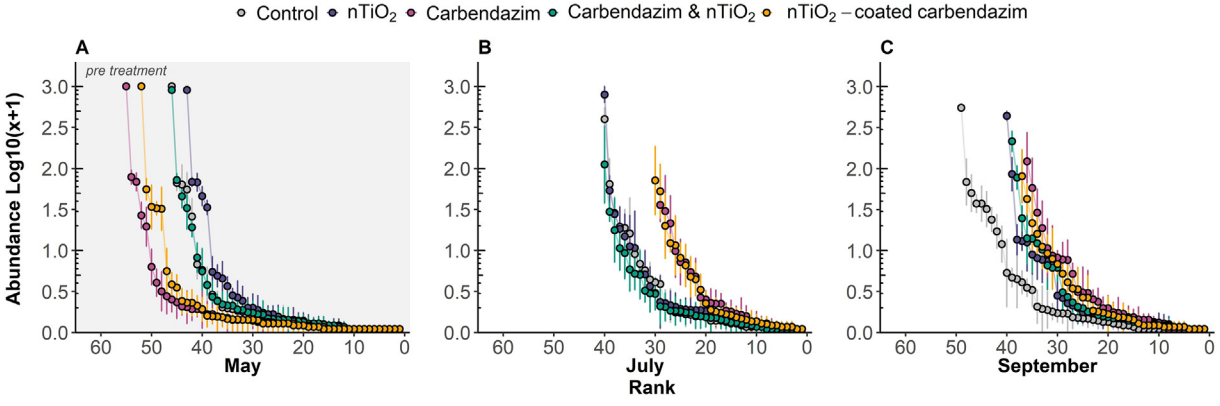

Fig. 4. Rank abundance curves (RACs) (mean ± standard error) per treatment and month generated using log10 (x + 1) transformed abundance data. May = 1 month pre-treatment application, July = 1 month post treatment application and September = 3 months post treatment application.

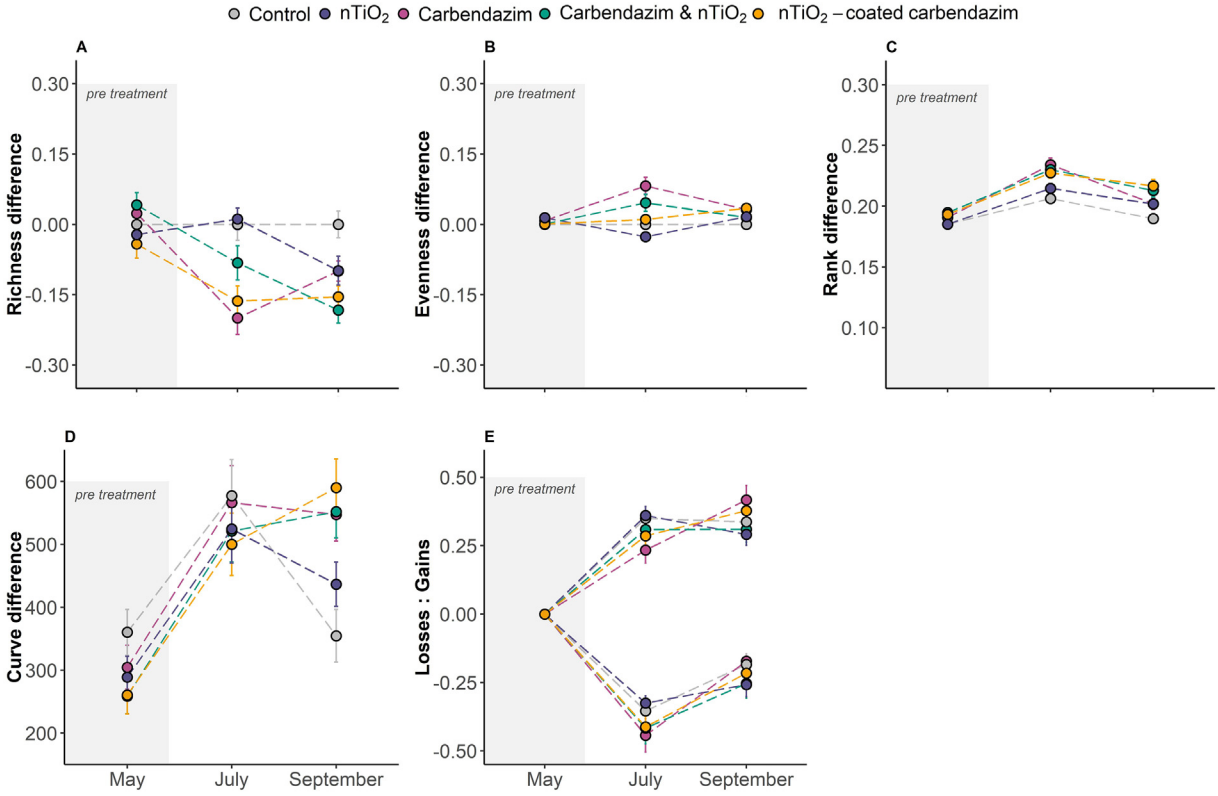

Fig. 5. Rank abundance curve (RAC) parameters (mean ± standard error) per treatment/month. In panel E, losses are indicated with negative values and gains are indicated with positive values. May = 1 month pre-treatment application, July = 1 month post treatment application and September = 3 months post treatment application.

showed comparable patterns for all carbendazim-including treatments (SI Table I2, SI Fig. I1). The two taxa which occupied the highest position in controls in July and September (i.e. Gammarids and Corixinae) shifted in position by a maximum of one step in all treatments. Other taxa showed more pronounced shifts however, including in particular Sialidae (negative shifts in position 3–18) and *Cloeon dipterum* (negative shifts in position 5–13) in July, and *Asellus aquaticus* (negative shifts in position 3–6) in September (SI Table I2, SI Fig. I1).

RACs of $nTiO_2$ treatments and controls were highly comparable (Figs. 4 & 5). The only difference from controls in this regard was found for taxonomic richness in September, which exhibited a (non-statistically significant) decrease (Tukey $p = 0.08$) relative to controls (Figs. 4C & 5A). The analysis of species abundance distributions (such as described by RACs) has been extensively discussed in fundamental ecological research for over 70 years, and more recently received recognition as an accurate and intuitive approach towards describing community responses to disturbances in applied ecological studies (Matthews and Whittaker, 2015). Avolio et al. (2019) indicate that taxonomic reordering is likely to be a larger driver of community change than turnover (as was also found in the current experiment), and in addition would be overlooked by merely focusing on β-diversity metrics. Results of the current experiment suggest that carbendazim and $nTiO_2$-coated carbendazim treatments affected both taxonomic reordering and β-diversity metrics, and overall effects were highly comparable between both treatments.

3.3.3. Biomass distribution across functional traits: feeding guilds & trophic groups

The distribution of biomass over functional traits such as feeding guilds and trophic groups provides a bridge between taxonomic composition and ecological functioning. Macroinvertebrate communities in the experimental setup were dominated by gatherer/collectors, shredders and grazers belonging predominantly to herbivorous and detritivorous (and thus omnivorous) trophic groups (Fig. 6). Statistically significant differences in biomass per functional trait were only observed three months after treatment applications (September), and as found for other measures of community composition, were limited to $nTiO_2$-coated carbendazim, carbendazim and combined treatments. This included a reduction in absolute biomass of shredders ($nTiO_2$-coated carbendazim: Dunnett $p = 8.0e^{-3}$; carbendazim: Dunnett $p = 0.04$; combined: Dunnett $p = 0.02$), grazers ($nTiO_2$-coated carbendazim: Dunnett $p = 2.1e^{-3}$; carbendazim: Dunnett $p = 0.04$; combined: Dunnett $p = 0.18$) and gatherers/collectors ($nTiO_2$-coated carbendazim: Dunnett $p = 6.1e^{-3}$; carbendazim: Dunnett $p = 0.08$; combined: Dunnett $p = 0.32$) (Fig. 6). These differences from controls were represented in the absolute biomass per trophic group as well, although only in $nTiO_2$-coated carbendazim and combined treatments ($nTiO_2$-coated carbendazim: Dunnett $p = 5.7e^{-3}$; carbendazim: Dunnett $p = 0.11$; combined: Dunnett $p = 0.03$). When expressed relative to the total biomass of the community, no differences between treatments and controls for any of the measured functional traits were observed (SI Table J1). This may partly be attributed to the dominance of the most affected functional groups in the experimental setup, but also indicates that overall, communities in all treatments displayed similar distributions of biomass across trait modalities. Nonetheless, it should be noted that specifically shredders, grazers and gatherers/collectors showed a substantial response to all carbendazim-including treatments, and that this suggests the possibility of cascading effects at the level of ecosystem functioning.

Functional groups in ecological communities are aggregates of taxa which occupy overlapping niches. Although the distribution of biomass over functional traits provides a relevant measure of community-level effects the perspective of ecological functioning, it thus inherently exhibits lower sensitivity than measures at lower levels of organization (i.e. individual taxa). This is particularly the case when community differences arise from effects on lesser abundant taxa, such as observed one month after treatment application (July) in the current experiment. As such, the absence of differences in biomass distributions between treatments and controls in July on the one hand, and the presence of differences in

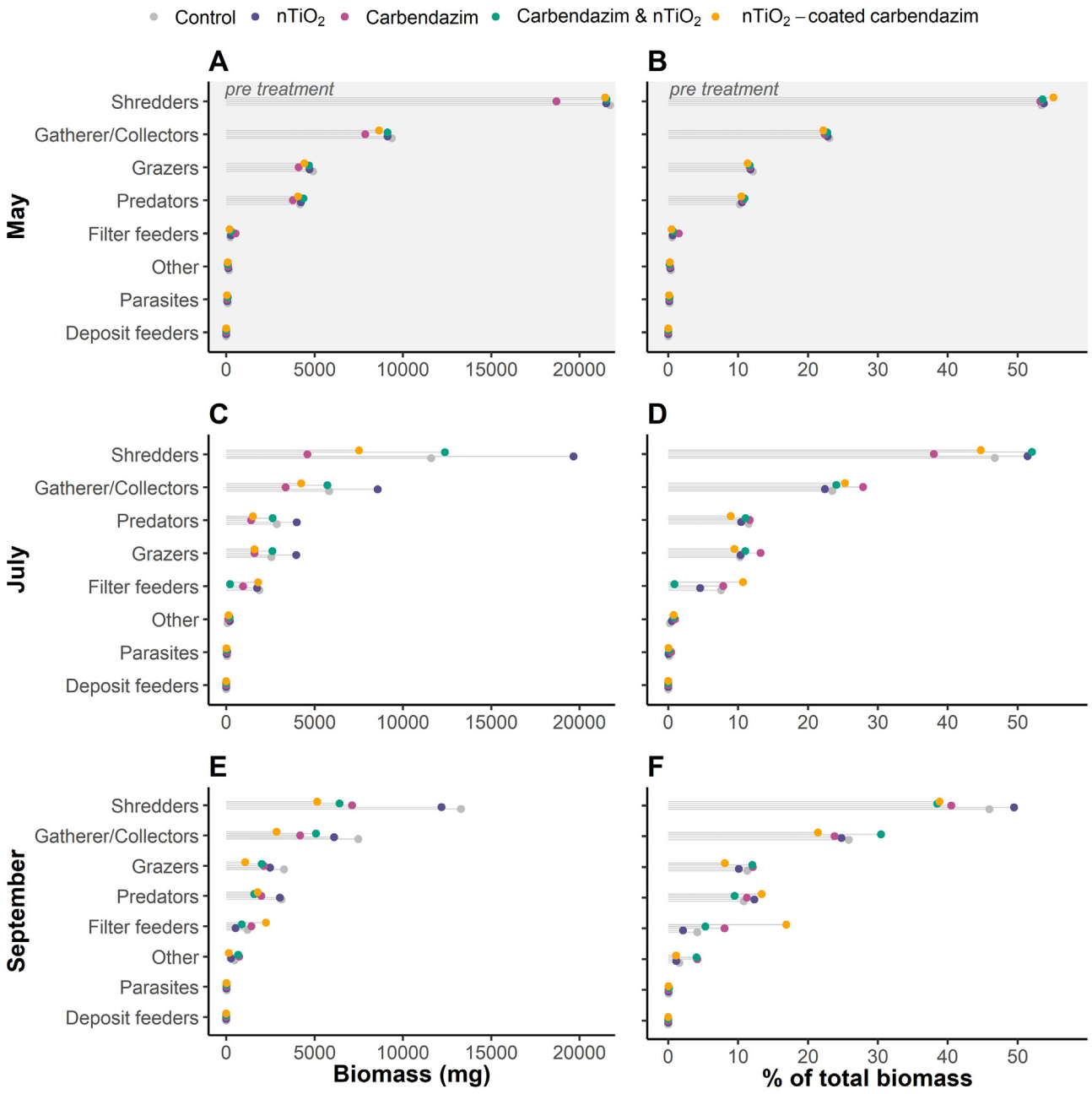

Fig. 6. Mean absolute- (A, C, E) and relative (B, D, F) biomass per feeding guild, treatment and month. May = 1 month pre-treatment application, July = 1 month post treatment application and September = 3 months post treatment application.

September on the other, are in concurrence with observations from community dissimilarity as discussed with regard to β-diversity indices (Section 3.3.1).

3.3.4. Impacts of $nTiO_2$-coated carbendazim on macroinvertebrate communities and differences from conventional carbendazim

Our results indicate that $nTiO_2$-coated carbendazim as synthesized for the purpose of the experiment induced quantitatively and qualitatively similar effects to conventional (i.e. un-coated) carbendazim (including when applied together with $nTiO_2$) at all evaluated levels of biological and ecological organization. Impacts of carbendazim were found to be more pronounced than observed at similar test concentrations in smaller scale studies which have been performed to date (Daam et al., 2009; Cuppen et al., 2000; Van den Brink et al., 2000). This builds on previous observations of impacts of other stressors in the applied experimental setup, and indicates that the inclusion of natural (re)colonizing communities in ecotoxicological studies allows for a realistic and sensitive evaluation of macroinvertebrate community dynamics.

3.3.5. Impacts of environmentally realistic concentrations of $nTiO_2$ on macroinvertebrate communities

The results of the current experiment show minimal impacts of an environmentally realistic concentration of $nTiO_2$ on all measured macroinvertebrate community parameters, which is in concordance with risk characterizations derived from available toxicity data and modelled environmental concentrations (Hong et al., 2021; Wigger & Nowack 2019, Coll et al., 2016). To our knowledge, only a single study assessed impacts of $nTiO_2$ on freshwater macroinvertebrate communities to date (Jovanović et al., 2016). In contrast to the present study, Jovanović et al. (2016) however focused on colonization rates of benthic macroinvertebrates in $nTiO_2$ spiked sediment (25 mg kg^{-1}), and found impacts on abundances of taxa and composition of colonizing communities. Crucially,

exposure pathways and concentrations differed between both experiments, and the current study considered impacts on both benthic and pelagic taxa which were already present prior to application of $nTiO_2$. As such, findings of both studies may best be considered as complementary rather than contradictive, and whether benthic communities indeed exhibit higher sensitivity to $nTiO_2$ than pelagic communities remains undetermined.

4. Conclusions and outlook

In the present study, we aimed to assess impacts of a novel controlled-release (nano-)pesticide formulation and its constituents on freshwater macroinvertebrate communities. The (nano-)formulation synthesized for the purpose of the experiment significantly delayed the release of carbendazim into the water column. Nevertheless, all carbendazim including treatments were found to induce fundamental restructuring of the taxonomic- and functional composition of macroinvertebrate communities, and effects of the controlled-release (nano-) formulation showed strong similarity to those of conventional (i.e. uncoated-) carbendazim for all measured community parameters. As such, no additional- or mitigating effects of the controlled-release (nano-) formulation were observed in this regard.

It should be noted that controlled-release formulations (and nano-pesticides) constitute a catch-all term, and that in the case of different active ingredients or altered properties (e.g. delaying release rates further than achieved in the current study), both efficacy in terms of pest control and adverse environmental impacts may vary. We therefore argue that in order to contribute to the reduction of pesticide pressures on freshwater ecosystems, the development of controlled-release (nano-)pesticide formulations should focus on iterative optimization of their properties. Thereby, these innovations may contribute to meeting safety and sustainability targets for NMs and NM-enabled products as proposed in the European Green Deal (European Commission, 2019).

Credit authorship contribution statement

TN: Conceptualization; Investigation; Methodology; Conceptualization; Data curation; Formal analysis; Visualization; Interpretation; Writing - original draft; WP: Conceptualization; Supervision; Funding Acquisition; Interpretation; Writing-review & editing; MV: Conceptualization; Supervision; Resources; Funding acquisition; Project administration; Interpretation; Writing-review & editing; RO Resources; Interpretation; Writing-review & editing; MS: Interpretation; Writing-review & editing.

Declaration of competing interest

The authors declare that they have no known competing financial interests or personal relationships that could have appeared to influence the work reported in this paper.

Acknowledgements

This work was supported by the project PATROLS, which is part of the European Union's Horizon 2020 research and innovation programme [grant number 760813]. We thank the Joint Research Centre (JRC) for providing the $nTiO_2$ used in the experiment, Damiano La Zara for preparing the $nTiO_2$-coated carbendazim and Yuyang Tian for carrying out the lab-based release experiments. We would like to express our gratitude towards all volunteers, employees and students who assisted in the practical work, including in particular MSc. students Bo Bode, Bob Bastiaan and Richard Frische.

Appendix A. Supplementary data

Supplementary data to this article can be found online at https://doi.org/10.1016/j.scitotenv.2022.156554.

References

Albert, J.S., Destouni, G., Duke-Sylvester, S.M., Magurran, A.E., Oberdorff, T., Reis, R.E., Winemiller, K.O., Ripple, W.J., 2021. Scientists' warning to humanity on the freshwater biodiversity crisis. Ambio 50 (1), 85–94. https://doi.org/10.1007/s13280-020-01318-8.

Alejandro, M.N.M., Guadalupe, B.E., Omar, T.S.F., Patricia, R.R., 2022. Temporal and spatial analysis of benomyl/carbendazim in water and its possible impact on Nile tilapia (Oreochromis niloticus) from Tenango dam, Puebla, Mexico. Environ. Monit. Assess. 194 (1),), 1–), 13. https://doi.org/10.1007/s10661-021-09661-3.

Anderson, M.J., Walsh, D.C., 2013. PERMANOVA, ANOSIM, and the mantel test in the face of heterogeneous dispersions: what null hypothesis are you testing? Ecol. Monogr. 83 (4), 557–574. https://doi.org/10.1890/12-2010.1.

Anderson, M.J., Crist, T.O., Chase, J.M., Vellend, M., Inouye, B.D., Freestone, A.L., Sanders, N.J., Cornell, H.V., Comita, L.S., Davies, K.F., Harrison, S.P., Kraft, N.J.B., Stegen, J.C., Swenson, N.G., 2011. Navigating the multiple meanings of β diversity: a roadmap for the practicing ecologist. Ecol. 14 (1), 19–28. https://doi.org/10.1111/j.1461-0248.2010.01552.x.

Arthington, A.H., 2021. Grand challenges to support the freshwater biodiversity emergency recovery plan. Front. Environ. Sci. 9, 118. https://doi.org/10.3389/fenvs.2021.664313.

Avolio, M.L., Carroll, I.T., Collins, S.L., Houseman, G.R., Hallett, L.M., Isbell, F., Koerner, S.E., Komatsu, K.J., Smith, M.D., Wilcox, K.R., 2019. A comprehensive approach to analyzing community dynamics using rank abundance curves. Ecosphere 10 (10), e02881. https://doi.org/10.1002/ecs2.2881.

Avolio, M.L., Komatsu, K.J., Collins, S.L., Grman, E., Koerner, S.E., Tredennick, A.T., Wilcox, K.R., Baer, S., Boughton, E.H., Britton, A.J., Foster, B., Gough, L., Hovenden, M., Isbell, F., Jentsch, A., Johnson, D.S., Knapp, A.K., Kreyling, J., Langley, J.A., Lortie, C., McCulley, R.L., McLaren, J.R., Reich, J.B., Seabloom, E.W., Smith, M.D., Suding, K.N., Suttle, B., Tognetti, P.M., 2021. Determinants of community compositional change are equally affected by global change. Ecol. Lett. 24 (9), 1892–1904. https://doi.org/10.1111/ele.13824.

Barmentlo, 2020. Neonicotinoids in Nature: The Effects on Aquatic Invertebrates and Their Role in Ecosystems. Leiden University. https://hdl.handle.net/1887/138079.

Barmentlo, S.H., Schrama, M., van Bodegom, P.M., de Snoo, G.R., Musters, C.J.M., Vijver, M.G., 2019. Neonicotinoids and fertilizers jointly structure naturally assembled freshwater macroinvertebrate communities. Proc. Natl. Acad. Sci. U. S. A. 691, 36–44. https://doi.org/10.1016/j.scitotenv.2019.07.110.

Barmentlo, S.H., Schrama, M., De Snoo, G.R., Van Bodegom, P.M., van Nieuwenhuijzen, A., Vijver, M.G., 2021. Experimental evidence for neonicotinoid driven decline in aquatic emerging insects. PNAS 118 (44). https://doi.org/10.1073/pnas.2105692118.

Beentjes, K.K., Barmentlo, S.H., Cieraad, E., Schilthuizen, M., van der Hoorn, B.B., Speksnijder, A.G., Trimbos, K.B., 2021. Environmental DNA metabarcoding reveals comparable responses to agricultural stressors on different trophic levels of a freshwater community. Mol. Ecol. https://doi.org/10.1111/mec.16326.

BKMW: Besluit kwaliteitseisen en monitoring water, 2009. https://wetten.overheid.nl/BWBR0027061/2017-01-01 (Accessed March 2022).

Brühl, C.A., Zaller, J.G., 2019. Biodiversity decline as a consequence of an inappropriate environmental risk assessment of pesticides. Front. Environ. Sci. 177. https://doi.org/10.3389/fenvs.2019.00177.

Brunelli, A., Pojana, G., Callegaro, S., Marcomini, A., 2013. Agglomeration and sedimentation of titanium dioxide nanoparticles (n-TiO2) in synthetic and real waters. J. Nanopart. Res. 15 (6), 1–10. https://doi.org/10.1007/s11051-013-1684-4.

Clement, W.H., Hickey, C.W., Kidd, K., 2012. How do aquatic communities respond to contaminants? It depends on the ecological context. Environ. Toxicol. Chem. 31, 1932–1940. https://doi.org/10.1002/ect.1937.

Clément, L., Hurel, C., Marmier, N., 2013. Toxicity of TiO2 nanoparticles to cladocerans, algae, rotifers and plants–effects of size and crystalline structure. Chemosphere 90 (3), 1083–1090. https://doi.org/10.1016/j.chemosphere.2012.09.013.

Coll, C., Notter, D., Gottschalk, F., Sun, T., Som, C., Nowack, B., 2016. Probabilistic environmental risk assessment of five nanomaterials (nano-TiO2, nano-Ag, nano-ZnO, CNT, and fullerenes). Nanotoxicology 10 (4), 436–444. https://doi.org/10.3109/17435390.2015.1073812.

Collen, B., Loh, J., Whitmee, S., McRae, L., Amin, R., Baillie, J.E.M., 2009. Monitoring change in vertebrate abundance: the Living Planet Index. Conserv. Biol. 23, 317–327. https://doi.org/10.1111/j.1523-1739.2008.01117.x.

Crutzen, P.J., 2006. The "anthropocene". Earth System Science in the Anthropocene. Springer, Berlin, Heidelberg, pp. 13–18 https://doi.org/10.1007/3-540-26590-2_3.

Cuppen, J.G., Van den Brink, P.J., Camps, E., Uil, K.F., Brock, T.C., 2000. Impact of the fungicide carbendazim in freshwater microcosms. I. Water quality, breakdown of particulate organic matter and responses of macroinvertebrates. Aquat. Toxicol. 48 (2–3), 233–250. https://doi.org/10.1016/S0166-445X(99)00036-3.

Daam, M.A., Satapornvanit, K., Van den Brink, P.J., Nogueira, A.J., 2009. Sensitivity of macroinvertebrates to carbendazim under semi-field conditions in Thailand: implications for the use of temperate toxicity data in a tropical risk assessment of fungicides. Chemosphere 74 (9), 1187–1194. https://doi.org/10.1016/j.chemosphere.2008.11.040.

European Commission, 2019. Communication From the Commission to the European Parliament, the European Council, the Council, the European Economic and Social Committee and the Committee of the Regions–The European Green Deal. Document 52019DC0640. 640.

European Commission, 2020. Report From the Commission to the European Parliament and the Council on the Experience Gained by Member States on the Implementation of National Targets Established in Their National Action Plans and on Progress in the Implementation of Directive 2009/128/EC on the Sustainable Use of Pesticides. Brussels, 20.5.2020 COM(2020). 204.

Grillo, R., Fraceto, L.F., Amorim, M.J., Scott-Fordsmand, J.J., Schoonjans, R., Chaudhry, Q., 2021. Ecotoxicological and regulatory aspects of environmental sustainability of

nanopesticides. J. Hazard. Mater. 404, 124148. https://doi.org/10.1016/j.jhazmat.2020.124148.
Hong, H., Adam, V., Nowack, B., 2021. Form-specific and probabilistic environmental risk assessment of 3 engineered nanomaterials (nano-Ag, nano-TiO2, and nano-ZnO) in European freshwaters. Environ. Toxicol. Chem. 40 (9), 2629–2639. https://doi.org/10.1002/etc.5146.
IPBES, 2019. Summary for policymakers of the global assessment report of the intergovernmental science-policy platform on biodiversity and ecosystem services. In: Díaz, S., Settele, J., Brondízio, E.S., Ngo, H.T., Guèze, M., Agard, J., Arneth, A., Balvanera, P., Brauman, K.A., Butchart, S.H.M., Chan, K.M.A., Garibaldi, L.A., Ichii, K., Liu, J., Subramanian, S.M., Midgley, G.F., Miloslavich, P., Molnár, Z., Obura, D., Pfaff, A., Polasky, S., Purvis, A., Razzaque, J., Reyers, B., Chowdhury, R. Roy, Shin, Y.J., Visseren-Hamakers, I.J., Willis, K.J., Zayas, C.N. (Eds.), Bonn, Germany: Secretariat of the Intergovernmental Platform for Biodiversity and Ecosystem Services.
Jovanović, B., Bezirci, G., Çağan, A.S., Coppens, J., Levi, E.E., Oluz, Z., Tuncel, E., Duran, H., Beklioğlu, M., 2016. Food web effects of titanium dioxide nanoparticles in an outdoor freshwater mesocosm experiment. Nanotoxicology 10 (7), 902–912. https://doi.org/10.3109/17435390.2016.1140242.
JRC, 2014. Titanium Dioxide, NM-100, NM-101, NM-102, NM-103, NM-104, NM-105: Characterisation and Physico-Chemical Properties. JRC Science and Policy Reports, JRC 86291.
Kääriäinen, T.O., Kemell, M., Vehkamäki, M., Kääriäinen, M.L., Correia, A., Santos, H.A., Bimbo, L.M., Hirvonen, J., Hoppu, P., George, S.M., Cameron, D.C., Ritala, M., Leskelä, M., 2017. Surface modification of acetaminophen particles by atomic layer deposition. Int. J. Pharm. 525 (1), 160–174. https://doi.org/10.1016/j.ijpharm.2017.04.031.
Kah, M., Tufenkji, N., White, J.C., 2019. Nano-enabled strategies to enhance crop nutrition and protection. Nat. Nanotechnol. 14 (6), 532–540. https://doi.org/10.1038/s41565-019-0439-5.
La Zara, D., Sun, F., Zhang, F., Franek, F., Balogh Sivars, K., Horndahl, J., Bates, S., Bränstörm, M., Ewing, P., Quayle, M.J., Petersson, G., Folestad, S., van Ommen, J.R., 2021. Controlled pulmonary delivery of carrier-free budesonide dry powder by atomic layer deposition. ACS Nano 15 (4), 6684–6698. https://doi.org/10.1021/acsnano.0c10040.
Maasri, A., Jähnig, S.C., Adamescu, M.C., Adrian, R., Baigun, C., Baird, D.J., et al., 2022. A global agenda for advancing freshwater biodiversity research. Ecol. Lett. 25, 255–263. https://doi.org/10.1111/ele.13931.
Matthews, T.J., Whittaker, R.J., 2015. On the species abundance distribution in applied ecology and biodiversity management. J. Appl. Ecol. 52 (2), 443–454. https://doi.org/10.1111/1365-2664.12380.
Merel, S., Benzing, S., Gleiser, C., Di Napoli-Davis, G., Zwiener, C., 2018. Occurrence and overlooked sources of the biocide carbendazim in wastewater and surface water. Environ. Pollut. 239, 512–521. https://doi.org/10.1016/j.envpol.2018.04.040.
Zheng, Y., Nowack, B., 2021. Size-specific, dynamic, probabilistic material flow analysis of titanium dioxide releases into the environment. Environ. Sci. Technol. 55 (4), 2392–2402. https://doi.org/10.1021/acs.est.0c07446.
Mesocosm.org, n.d.Mesocosm.org (n.d.): an information hub of MESOcosm facilities in AQUAtic ecosystems worldwide. Accessed March 2022.
Nabi, M.M., Wang, J., Goharian, E., Baalousha, M., 2022. Temporal variation in TiO2 engineered particle concentrations in the Broad River during dry and wet weathers. Sci. Total Environ. 807, 151081. https://doi.org/10.1016/j.scitotenv.2021.151081.
Nederstigt, T.A.P., Peijnenburg, W.J., Bleeker, E.A., Vijver, M.G., 2022. Applicability of nanomaterial-specific guidelines within long-term Daphnia magna toxicity assays: a case study on multigenerational effects of nTiO2 and nCeO2 exposure in the presence of artificial daylight. Regul. Toxicol. Pharmacol. 105156. https://doi.org/10.1016/j.yrtph.2022.105156.
OECD, 2017. Test No. 318: Dispersion Stability of Nanomaterials in Simulated Environmental Media, OECD Guidelines for the Testing of Chemicals, Section 3. OECD Publishing, Paris https://doi.org/10.1787/9789264284142-en.
OECD, 2021. Guidance Document No. 317: Guidance Document on Aquatic and Sediment Toxicological Testing of Nanomaterials, Series on Testing and Assessment. OECD Publishing, Paris.
Persson, L., Carney Almroth, B.M., Collins, C.D., Cornell, S., de Wit, C.A., Diamond, M.L., Fantke, P., Hassellöv, M., MacLeod, M., Ryberg, M.W., Søgaard Jørgensen, P., Villarrubia-Gómez, P., Wang, Z., Hauschild, M.Z., 2022. Outside the safe operating space of the planetary boundary for novel entities. Environ. Sci. Technol. 56 (3), 1510–1521. https://doi.org/10.1021/acs.est.1c04158.
Peters, R.J., van Bemmel, G., Milani, N.B., den Hertog, G.C., Undas, A.K., van der Lee, M., Bouwmeester, H., 2018. Detection of nanoparticles in dutch surface waters. Sci. Total Environ. 621, 210–218. https://doi.org/10.1016/j.scitotenv.2017.11.238.
R Core Team, 2017. R: A Language and Environment for Statistical Computing. . https://www.R-project.org/.
Reid, A.J., Carlson, A.K., Creed, I.F., Eliason, E.J., Gell, P.A., Johnson, P.T., Kidd, K.A., MacCormack, T.J., Olden, J.D., Ormerod, S.J., Smol, J.P., Taylor, W.W., Tockner, K., Vermaire, J.C., Dugeon, D., Cooke, S.J., 2019. Emerging threats and persistent conservation challenges for freshwater biodiversity. Biol. Rev. Biol. Proc. Camb. Philos. Soc. 94 (3), 849–873. https://doi.org/10.1111/brv.12480.
Sabo, J.L., Bastow, J.L., Power, M.E., 2002. Length–mass relationships for adult aquatic and terrestrial invertebrates in a California watershed. J. North Am. Benthol. Soc. 21 (2), 336–343. https://doi.org/10.2307/1468420.
Schmidt-Kloiber, A., Hering, D., 2015. www.Freshwaterecology.Info - an online tool that unifies, standardises and codifies more than 20,000 European freshwater organisms and their ecological preferences. Ecol. Indic. 53, 271–282. https://doi.org/10.1016/j.ecolind.2015.02.007.
Scott-Fordsmand, J.J., Fraceto, L.F., Amorim, M.J.B., 2022. Nano-pesticides: the lunch-box principle—deadly goodies (semio-chemical functionalised nanoparticles that deliver pesticide only to target species). J. Nanobiotechnology. 20 (1), 1–9. https://doi.org/10.1186/s12951-021-01216-5.
Socolar, J.B., Gilroy, J.J., Kunin, W.E., Edwards, D.P., 2016. How should beta-diversity inform biodiversity conservation? Trends Ecol. Evol. 31 (1), 67–80. https://doi.org/10.1016/j.tree.2015.11.005.
Sun, Y., Liang, J., Tang, L., Li, H., Zhu, Y., Jiang, D., Song, B., Chen, B., Zeng, G., 2019. Nanopesticides: a great challenge for biodiversity? Nano Today 28, 100757. https://doi.org/10.1016/j.nantod.2019.06.003.
Tebby, C., Joachim, S., Van den Brink, P.J., Porcher, J.M., Beaudouin, R., 2017. Analysis of community-level mesocosm data based on ecologically meaningful dissimilarity measures and data transformation. Environ. Toxicol. Chem. 36 (6), 1667–1679. https://doi.org/10.1002/etc.3701.
Van den Brink, P.J., Hattink, J., Bransen, F., Van Donk, E., Brock, T.C., 2000. Impact of the fungicide carbendazim in freshwater microcosms. II. Zooplankton, primary producers and final conclusions. Aquat. Toxicol. 48 (2–3), 251–264. https://doi.org/10.1016/S0166-445X(99)00036-3.
Wan, Y., Tran, T.M., Nguyen, V.T., Wang, A., Wang, J., Kannan, K., 2021. Neonicotinoids, fipronil, chlorpyrifos, carbendazim, chlorotriazines, chlorophenoxy herbicides, bentazon, and selected pesticide transformation products in surface water and drinking water from northern Vietnam. Sci. Total Environ. 750, 141507. https://doi.org/10.1016/j.scitotenv.2020.141507.
Wang, X., Li, S., Huang, S., Cui, Y., Fu, H., Li, T., Zhao, W., Yang, X., 2021. Pinus massoniana population dynamics: driving species diversity during the pioneer stage of ecological restoration. Glob. Ecol. 27, e01593. https://doi.org/10.1016/j.gecco.2021.e01593.
WHO Working Group, 1993. Carbendazim. Environmental Health Criteria, 149, 132. Report number RISKLINE/1994010028. HERO ID: 1809680.
Wigger, H., Nowack, B., 2019. Material-specific properties applied to an environmental risk assessment of engineered nanomaterials–implications on grouping and read-across concepts. Nanotoxicology 13 (5), 623–643. https://doi.org/10.1080/17435390.2019.1568604.
Yan, X., Chen, X., 2015. Titanium dioxide nanomaterials. Encyclopedia of Inorganic and Bioinorganic Chemistry. 1–38. https://doi.org/10.1002/9781119951438.eibc2335.
Zhang, D., La Zara, D., Quayle, M.J., Petersson, G., Van Ommen, J.R., Folestad, S., 2019. Nanoengineering of crystal and amorphous surfaces of pharmaceutical particles for biomedical applications. ACS Appl. Bio Mater. 2 (4), 1518–1530. https://doi.org/10.1021/acsabm.8b00805.
Zhang, P., Guo, Z., Ullah, S., Melagraki, G., Afantitis, A., Lynch, I., 2021. Nanotechnology and artificial intelligence to enable sustainable and precision agriculture. Nat. Plants 7 (7), 864–876. https://doi.org/10.1038/s41477-021-00946-6.